J|A|C|S
ARTICLES
Published on Web 01/09/2003

Crown-Annelated Oligothiophenes as Model Compounds for Molecular Actuation

Bruno Jousselme,[†] Philippe Blanchard,*[,†] Eric Levillain,[†] Jacques Delaunay,[‡] Magali Allain,[‡] Pascal Richomme,[§] David Rondeau,[§] Nuria Gallego-Planas,[‡] and Jean Roncali*[,†]

Contribution from Groupe Systèmes Conjugués Linéaires and Ingénierie Moléculaire et Matériaux Organiques, UMR CNRS 6501, and Service Commun d'Analyses Spectroscopiques, Université d'Angers, 2 Boulevard Lavoisier, 49045 Angers, France

Received May 7, 2002; E-mail: jean.roncali@univ-angers.fr

Abstract: Crown-annelated quater- (4T) and sexithiophenes (6T) with oligooxyethylene chains of various lengths attached at the 3-positions of the terminal thiophene rings have been synthesized. Analysis of the cation-binding properties of the macrocycles by ^{1}H NMR and UV−vis spectroscopy reveals the formation of a 1:1 complex with Ba^{2+}, Sr^{2+}, or Pb^{2+} and shows that cation complexation results in a conformational transition in the π-conjugated system. Theoretical analysis of this process by density functional methods predicts that this conformational transition results in a narrowing of the highest occupied−lowest unoccupied molecular orbital gap of the conjugated system with a decrease of the redox potentials (E^0_1 and E^0_2) associated with the formation of the 4T cation radical and dication. Cyclic voltammetry shows that, depending on the binding constant, the presence of metal cation produces a negative or a positive shift of E^0_1 while E^0_2 always shifts negatively. This unusual behavior is discussed in terms of interplay between electrostatic interactions and conformational changes associated with cation binding.

Introduction

Motion generation at the molecular level by means of chemical, electrochemical, or photochemical stimulation has recently become a focus of considerable interest in the general context of molecular machines.[1−6] Stoddart and co-workers[1b,2] have developed molecular shuttles in which change of the oxidation state of a redox system imbedded in a rotaxane induces its translocation along a linear axis. Sauvage and co-workers[1c,3,4] have synthesized molecular machines and molecular muscles powered by the modification of the coordination sphere of a metal involved in rotaxanes containing tetra- and pentacoordination sites. Photochemically powered molecular machines undergoing circular motion have been described by Feringa and co-workers,[5] while Gaub and co-workers[6] have investigated a polymeric system undergoing a single-molecule optomechanical cycle.

Thiophene-based monodisperse π-conjugated oligomers have much interest as active material in field effects transistors or light-emitting diodes.[7,8] Although these oligomers have also been considered as molecular wires for molecular electronic devices,[9] their possible use in dynamic nanosystems has been scarcely considered so far. Bulk electrochemical actuators based on the volume changes associated with the doping/undoping process of conjugated polymers have been known for some time,[10] but

* Corresponding authors.
[†] Groupe Systèmes Conjugués Linéaires.
[‡] Ingénierie Moléculaire et Matériaux Organiques.
[§] Service Commun d'Analyses Spectroscopiques.

(1) (a) Drexler, K. E. *Nanosystems: Molecular Machinery, Manufacturing and Computation*; Wiley, New York 1992. (b) Kelly, T. R.; De Silva, H.; Silva, R. A. *Nature* **1999**, *401*, 150. (b) Fyfe, M. C. T.; Stoddart, J. F. *Acc. Chem. Res.* **1997**, *30*, 393. (c) Sauvage, J.-P. *Acc. Chem. Res.* **1998**, *31*, 611. (d) Balzani, V.; Gomez-Lopez, M.; Stoddart, J. F. *31*, 405. (e) Koumura, N.; Zijlstra, R. W.; van Delden, R. A.; Harada, N.; Feringa, B. L. *Nature* **1999**, *401*, 152.
(2) Bissell, R. A.; Cordova, E.; Kaifer, A. E.; Stoddardt, J. F. *Nature* **1994**, *369*, 133.
(3) Livoreil, A.; Dietrich-Buchecker, C. O.; Sauvage, J.-P. *J. Am. Chem. Soc.* **1994**, *116*, 9399.
(4) Jimenez, M. C.; Dietrich-Buchecker, C.; Sauvage, J.-P.; DeCian, A. *Angew. Chem., Int. Ed.* **2000**, *39*, 1295.
(5) Koumura, N.; Zijistra, R. W. L.; van Delden, R. A.; Harada, N.; Feringa, B. L. *Nature* **1999**, *401*, 152
(6) Hugel, T.; Holland, N. B.; Cattani, A.; Moroder, L.; Markus, S.; Gaub, H. E. *Science* **2002**, *296*, 1103.
(7) (a) Dimitrakopoulos, C. D.; Malenfant, P. R. L. *Adv. Mater.* **2002**, *14*, 99. (b) Rogers, J. A.; Bao, Z.; Dodabalapur, A.; Crone, B.; Raju, V. R.; Katz, H. E.; Kuck, V.; Ammundson, K. J.; Drzaic, P. *Proc. Natl. Acad. Sci. U.S.A.* **2001**, *98*, 4817. (c) Garnier, F. *Acc. Chem. Res.* **1999**, *32*, 209. (d) Horowitz, G. *Adv. Mater.* **1998**, *10*, 3. (e) Katz, H. E. *J. Mater. Chem.* **1997**, *7*, 369. (f) Garnier, F.; Yassar, A.; Hajlaoui, R.; Horowitz, G.; Deloffre, F.; Servet, B.; Ries, S.; Alnot, P. *J. Am. Chem. Soc.* **1993**, *115*, 8716. (g) Barbarella, G.; Zambianchi, M.; Antolini, L.; Ostoja, P.; Maccagnani, P.; Bongini, A.; Marseglia, E. A.; Tedesco, E.; Gigli, G.; Cingolani, R. *J. Am. Chem. Soc.* **1999**, *121*, 8920.
(8) (a) Geiger, F.; Stoldt, M.; Schweiser, R.; Bäuerle, P.; Umbach, E. *Adv. Mater.* **1993**, *5*, 922. (b) Barbarella, G.; Favaretto, L.; Sotgiu, G.; Zambianchi, P.; Bongini, A.; Arbizzani, C.; Mastragostino, M.; Anni, M.; Gigli, G.; Cingolani, R. *J. Am. Chem. Soc.* **2000**, *122*, 11971. (c) Barbarella, G.; Favaretto, L.; Sotgiu, G.; Antolini, L.; Gigli, G.; Cingolani, R.; Bongini, A. *Chem. Mater.* **2001**, *13*, 4112.
(9) (a) Aviram, A. *J. Am. Chem. Soc.* **1988**, *110*, 5687. (b) Guay, J.; Diaz, A.; Wu, R.; Tour, J. M. *J. Am. Chem. Soc.* **1993**, *115*, 1869. (c) Wu, R.; Schumm, J. S.; Pearson, D. L.; Tour, J. M. *J. Org. Chem.* **1996**, *61*, 6906. (d) Kergueris, C.; Bourgoin, J.-P.; Palacin, S.; Esteve, D.; Urbina, C.; Magoga, M.; Joachim, C. *Phys. Rev. B* **1999**, *59*, 12505. (e) Roncali, J. *Acc. Chem. Res.* **2000**, *33*, 147. (f) Jestin, I.; Frère, P.; Blanchard, P.; Roncali, J. *Angew. Chem., Int. Ed.* **1998**, *37*, 942.(g) Jestin, I.; Frère, P.; Mercier, N.; Levillain, E.; Stiévenard, D.; Roncali, J. *J. Am. Chem. Soc.* **1998**, *120*, 8150.
(10) Baughman, R. H. *Synth. Met.* **1996**, *78*, 339.

the molecular parent systems are still to be developed. A first step in this direction was recently reported by Marsella et al.,[11] who reported a model of molecular actuator based on poly-[cyclooctatetrathiophene].

In this work we propose a different concept of molecular actuator in which stimulation of a driving group covalently attached at two fixed points of an oligothiophene chain is used to produce dimensional changes in the π-conjugated system. A particularly interesting aspect of this approach is that the π-conjugated system simultaneously constitutes the target of the generated movement and an optical and redox probe, allowing its real-time monitoring by simple electrochemical and optical techniques.

Derivatization of poly(thiophenes) by linear or macrocyclic polyethers has been widely investigated in view of developing ion sensors.[12−15] Whereas most of these systems are based on the changes induced in the electrochemical response of the π-conjugated system by electrostatic interactions between the metal cation and the oxidized π-conjugated system,[13] some examples are known where cation binding induces geometrical changes in the conjugated chain.[14,15]

We show here that cation complexation can be used as the driving force to produce geometrical changes in a conjugated oligothiophene (*n*T) and hence to design single-molecule electromechanical actuators.

To this end, two series of quarter- (4T) and sexithiophenes (6T) bearing oligooxyethylene loops of variable length have been synthesized. The ionophoric properties of these compounds have been analyzed in the presence of different metal cations by ^{1}H NMR and mass spectrometry, UV−vis absorption spectroscopy, and cyclic voltammetry. These investigations together with crystallographic and theoretical results provide a coherent picture showing that cation binding induces large conformational transitions in the π-conjugated chain, thus making these new systems interesting models of molecular actuators.

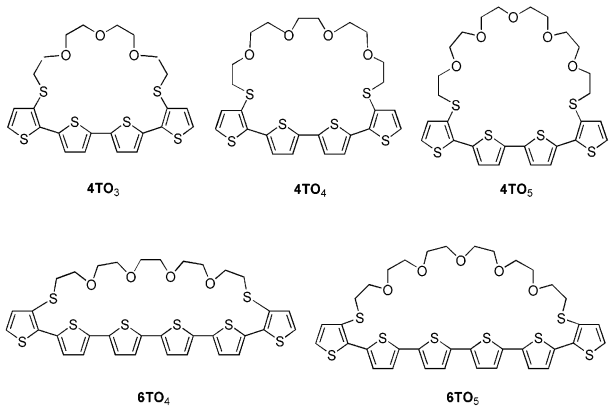

Results and Discussion

Synthesis. The crown-annelated 4Ts and 6Ts have been synthesized according to the procedure depicted in Scheme 1. Our strategy involves the preparation of an oligomer possessing two protected thiolate groups at the 3-positions of the terminal thiophene rings (**1**).[16] The target compounds are then obtained

Scheme 1

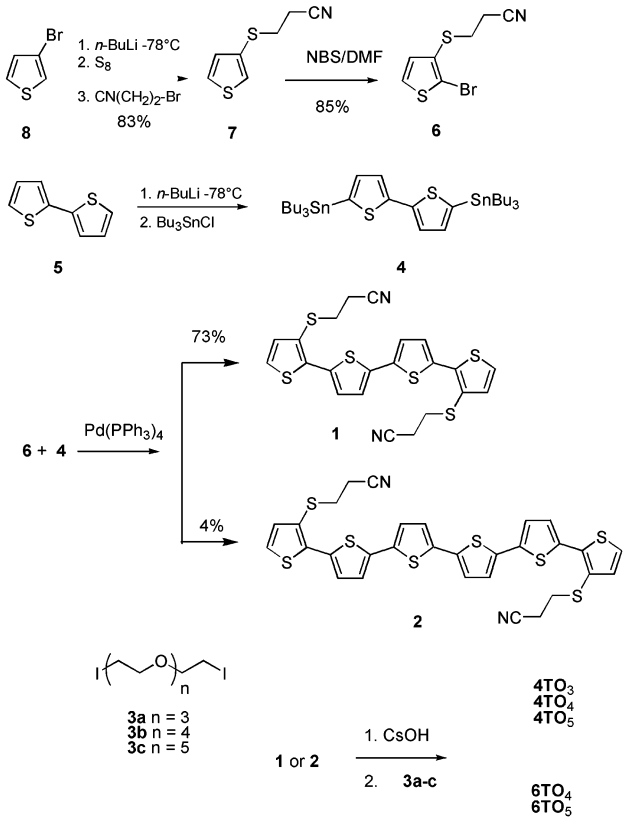

in one pot by deprotection of the thiolate functionality by cesium hydroxyde and ring closure by reaction with an α,ω-diiodo-oligooxyethylene chain under high dilution conditions. This methodology utilizes the chemistry developed by Becher and co-workers[17] for the synthesis of tetrathiafulvalene derivatives.

Successive treatments of commercially available 3-bromothiophene **8** with *n*-BuLi, elemental sulfur, and 3-bromopropionitrile give the key compound (2-cyanoethyl)sulfanylthiophene **7** in 83% yield. Selective bromination of **7** at the 2-position of thiophene with *N*-bromosuccinimide in DMF leads to the 2-bromothiophene derivative **6** in 90% yield. 5,5′-Bis(tributylstannyl)-2,2′-bithiophene **4** is obtained by treatment of bithiophene **5** with, successively, *n*-BuLi and tributylstannyl chloride.[18] The key compound 3,3‴-bis[(2-cyanoethyl)sulfanyl]-2,2′:5′,2″:5″,2‴-quaterthiophene **1** is then prepared by a double Stille coupling between distannyl bithiophene **4** and bromo compound **6** with $Pd(PPh_3)_4$ as catalyst. Treatment of a DMF solution of

(11) (a) Marsella, M. J.; Reid, R. J., *Macromolecules*, **1999**, *32*, 5982. (b) Marsella, M. J.; Reid, R. J.; Estassi, S.; Wang, L.-S. *J. Am. Chem. Soc.* **2002**, *124*, 12507.

(12) Reviews: (a) McQuade, D. T.; Pullen, A. E.; Swager, T. M. *Chem. Rev.* **2000**, *100*, 2537. (b) Roncali, J. *J. Mater. Chem.* **1999**, *9*, 1875.

(13) (a) Bäuerle, P.; Scheib, S. *Adv. Mater*. **1993**, *5*, 848. (b) Bäuerle, P.; Scheib, S. *Acta Polym.* **1995**, *46*, 124. (c) Rimmel, G.; Bäuerle, P. *Synth. Met.* **1999**, *102*, 1323. (d) Scheib, S.; Bäuerle, P. *J. Mater. Chem*. **1999**, *9*, 2139. (e) Sannicolò, F.; Brenna, E.; Benincori, T.; Zotti, G.; Zecchin, S.; Schiavon, G.; Pilati, T. *Chem. Mater*. **1998**, *10*, 2167.

(14) (a) Roncali, J.; Garreau, R.; Delabouglise, D.; Garnier, F.; Lemaire, M. *J. Chem. Soc., Chem. Commun.* **1989**, 679. (b) Roncali, J.; Shi, L. H.; Garnier, F. *J. Phys. Chem*. **1991**, *95*, 8983.

(15) (a) Marsella, M. J.; Swager, T. M. *J. Am. Chem. Soc.* **1993**, *115*, 12214. (b) Marsella, M. J.; Newland, R. J.; Carroll, P. J.; Swager, T. M. *J. Am. Chem. Soc.* **1995**, *11*, 7, 9842.

(16) (a) Blanchard, P.; Jousselme, B.; Frère, P.; Roncali, J. *J. Org. Chem.* **2002**, *67*, 3961. (b) Van Hal, P. A.; Beckers, E. H. A.; Meskers, S. C. J.; Janssen, R. A. J.; Jousselme, B.; Roncali, J. *Chem. Eur. J.* **2002**, *8*, 5415.

(17) (a) Svenstrup, N.; Rasmussen, K. M.; Hansen, T. K.; Becher, J. *Synthesis* **1994**, 809. (b) Becher, J.; Lau, J.; Leriche, P.; Mørk, P.; Svenstrup, N. *J. Chem. Soc., Chem. Commun*. **1994**, 2715. (c) Li, Z.-T.; Stein, P. C.; Svenstrup, N.; Lund, K. H.; Becher, J. *Angew. Chem., Int. Ed. Engl.*, **1995**, *34*, 2524.

(18) Wei, Y.; Yang, Y.; Yeh, J.-M. *Chem. Mater*. **1996**, *8*, 2659.

Table 1. Variation of ^{1}H NMR Chemical Shifts for **4TO$_4$** (9.56 mM) in 1:1 $CDCl_3/CD_3CN$ upon Addition of $Ba(ClO_4)_2$

equiv of Ba^{2+} added	$\Delta\delta_{H1}$[a]	$\Delta\delta_{H2}$[b]	$\Delta\delta_{H3'}$[c]	$\Delta\delta_{H4}$[d]
0.2	0.04	0.08	0.04	0.04
0.4	0.09	0.16	0.09	0.08
0.6	0.14	0.24	0.15	0.13
0.8	0.17	0.30	0.17	0.16
1.0	0.19	0.35	0.20	0.18
1.2	0.21	0.37	0.21	0.19
1.4	0.21	0.39	0.22	0.20
2.0	0.22	0.40	0.23	0.21

[a] Shifts are relative to $\delta_{H1} = 2.83$. [b] Shifts are relative to $\delta_{H2} = 3.34$. [c] Shifts are relative to $\delta_{H3'} = 3.25$. [d] Shifts are relative to $\delta_{H4} = 3.27$.

Chart 1

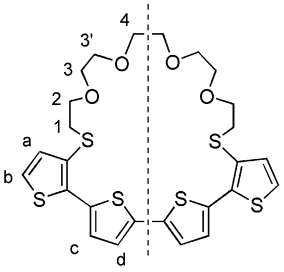

quaterthiophene **1** with 2.1 equiv of $CsOH\cdot H_2O$ in methanol, generates a dithiolate that is then reacted in situ with diiodo-oligooxyethylenes **3a**, **3b**, and **3c** under high dilution conditions to give the target quaterthiophenes **4TO$_3$**, **4TO$_4$**, and **4TO$_5$** in 34%, 47%, and 26% yields, respectively.

As already observed, the use of the Stille reaction for the synthesis of nTs leads to undesired homocoupling,[19] which results in our case in the formation of ca. 5% sexithiophene **2** during the synthesis of **1**. Since this compound could not be separated from **1**, the mixture of **1** and **2** was used in the next cyclization step, and crown-annelated sexithiophenes **6TO$_4$** and **6TO$_5$** were finally isolated in small amounts during the synthesis of their respective analogues **4TO$_4$** and **4TO$_5$**.

Ionophoric Properties of Crown-Annelated Oligothiophenes. The cation complexing properties of **4TO$_3$**, **4TO$_4$**, and **4TO$_5$** were first analyzed by ^{1}H NMR (500 MHz) titration experiments with solutions of Li^+, Na^+, and Ba^{2+} ions as perchlorate salts in 1:1 $CDCl_3/CD_3CN$. Alkali cations such as Li^+ and Na^+ have essentially no effect on the ^{1}H NMR spectrum. This absence of effect can be related to the inadequate geometry of the macrocyclic cavity and to the presence of two sulfur atoms in the macrocycle. In contrast, addition of substoichiometric amounts of Ba^{2+}, Sr^{2+}, or Pb^{2+} induces significant changes in the chemical shifts of various types of protons.

As shown in Table 1, the aliphatic protons of the polyether chain (Chart 1) shift downfield by 0.20−0.35 ppm, indicating that, as expected, complexation of Ba^{2+} essentially occurs within the macrocyclic cavity.

Table 2 lists the values of the binding constant (K^0) estimated by treatment of the data collected from the chemical shifts of H_1, H_2, H_3, and H_4 with the EQNMR program.[20] These results confirm that **4TO$_n$** do not complex alkali cations but form 1:1 complexes with low to moderate binding constants with alkali earth cations. The formation of a 1:1 complex is confirmed by

(19) Roth, G. P.; Farina, V.; Liebeskind, L. S.; Pena-cabrera, E. *Tetrahedron Lett.* **1995**, *36*, 2191.
(20) Hynes, M. J. *J. Chem. Soc., Dalton Trans.* **1993**, 311.

Table 2. ^{1}H NMR Complexation Data for Crown-Annelated Quaterthiophenes[a]

compd	cation	complex	K^0 (M^{-1})
4TO$_3$	Li^+, Na^+	no	
	Ba^{2+}	no	
4TO$_4$	Li^+, Na^+	no	
	Ba^{2+}	1:1	7200 ± 600
	Sr^{2+}	1:1	900 ± 200
	Pb^{2+}	1:1	$>10^5$
4TO$_5$	Li^+, Na^+, Cs^+	no	
	Ba^{2+}	1:1	$>10^5$
	Sr^{2+}	1:1	$\sim 10^4$
	Pb^{2+}	1:1	$>10^5$

[a] Complexation in $CD_3CN/CDCl_3$ + 1 equiv of metal cation.

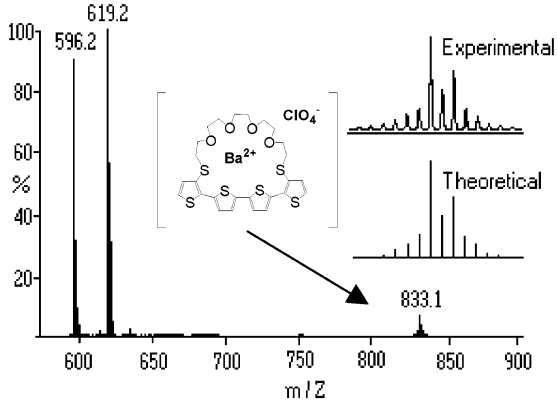

Figure 1. ESI mass spectrum of the 1:1 complex Ba^{2+}/**4TO$_4$**. Inset: experimental and calculated isotopic distributions for $[M + Ba(ClO_4)]^+$.

the occurrence of a net plateau around 1 equiv in the plot of the normalized chemical shifts of the protons of the poly(thio)-ether chain H_{1-4} versus the number of equivalents of metal cation. Definitive evidence for 1:1 complex formation is given by the mass spectrum of the **4TO$_4$**/Ba^{2+} complex, which exhibits the expected isotopic distribution (Figure 1).

As expected, the binding constant increases with the size of the macrocyclic cavity. Thus, whereas **4TO$_3$** shows no complexing properties, **4TO$_5$** exhibits the largest K^0 values. This result suggests that the longer oligooxyethylene loop of **4TO$_5$** allows a better adaptation of the size and geometry of the macrocyclic cavity to the size of the metal cation.

Figure 2 shows the chemical shifts of the aromatic thiophenic protons of the inner thiophenes. Whereas addition of 1 equiv of Ba^{2+} leaves the chemical shifts of the external H_a and H_b protons practically unchanged ($\Delta\delta_{Ha} = 0$ and $\Delta\delta_{Hb} = +0.03$ ppm for 5 equiv of Ba^{2+}), the progressive addition of small amounts of metal cation produces a positive shift of H_c but a negative shift of H_d.

These conflicting behaviors cannot be directly related to cation binding, since in that case the shift of both protons should have the same sign. This shows that cation complexation by the macrocyclic cavity indirectly produces a modification of the electronic environment of the protons of the inner thiophene rings. This result thus provide a first indication that cation binding by the macrocyclic cavity induces significant conformational changes in the π-conjugated 4T chain.

To better understand the relationships between the conformation and electronic properties of the annelated *n*Ts, a theoretical study has been undertaken. To this end, we first analyzed the crystallographic structure of single crystals of **4TO$_4$** and **6TO$_4$**

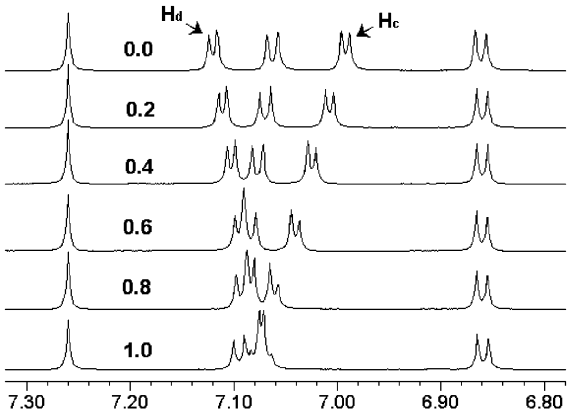

Figure 2. Changes in the chemical shifts of H_c and H_d aromatic protons (see Chart 1) of the central thiophenes of **4TO$_4$** in $CDCl_3/CD_3CN$ versus the number of equivalents of added Ba^{2+} from a solution of 0.20 M $Ba(ClO_4)_2$ in CD_3CN.

Table 3. Crystal Data and Structural Results for **6TO$_4$** and **4TO$_4$**

	6TO$_4$	4TO$_4$
chemical formula	$C_{34}H_{32}O_4S_8$	$C_{26}H_{28}O_4S_6$
formula weight (g/mol)	761.14	596.89
crystal size (mm^3)	1.23 × 0.69 × 0.06	1.29 × 0.11 × 0.09
crystal color	orange	yellow
crystal system	monoclinic	orthorhombic
space group	$P2_1$	$Pna2_1$
a (Å)	10.2317(9)	16.736(2)
b (Å)	8.1026(7)	21.481(4)
c (Å)	21.592(2)	7.788(1)
β (deg)	103.397(8)	
V ($Å^3$)	1741.3(5)	2799(1)
Z	2	4
2θ range (deg)	2.530	2.523
measured data	5681	2265
used data [$I > 3\sigma(I)$]	3232	865
no. of variables	406	174
R	0.048	0.065
Rw	0.064	0.080
GOF (goodness-of-fit)	1.221	1.470

grown by slow evaporation of 1:1 CH_3CN/CH_2Cl_2 (Table 3). Despite several attempts crystals of the metal containing macrocycles could not be obtained.

The numbering scheme and the molecular structure of the noncentrosymmetric **4TO$_4$** molecule are displayed in Figure 3. The π-conjugated system presents some departure from planarity; furthermore, the 4T chain contains two thiophene rings in a syn conformation, in striking contrast with the all-anti conformation usually observed for *n*Ts.[21] The torsional angles between the outer thiophene rings (C1, C2, C3, C4, S1) and (C13, C14, C15, C16, S4) and the neighboring thiophene rings are 33° and 22°, respectively. The torsional angle between the middle rings (C5, C6, C7, C8, S2) and (C9, C10, C11, C12, S3) is 18°. In the crystal structure, the shortest intermolecular S−S distance (d = 3.91 Å) is longer than the sum of the van der Waals radii; nevertheless, long C−H···S contacts (3.066 Å < d < 3.079 Å) and one short C−H···O contact (d = 2.54 Å) can be found between the molecules.

The structure of **6TO$_4$** (Figure 4) shows that the molecule is noncentrosymmetric and that the 6T chain also contains two

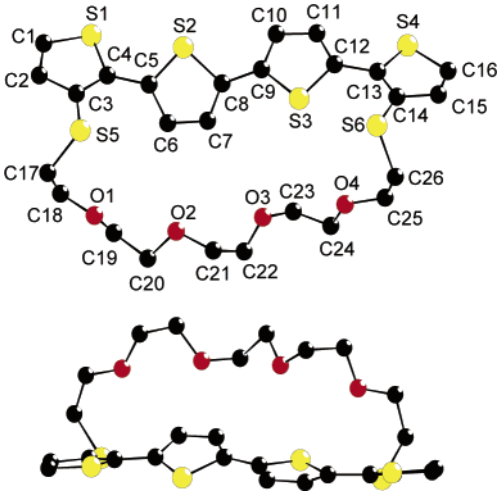

Figure 3. Crystal structure of 4**TO$_4$** (hydrogens omitted).

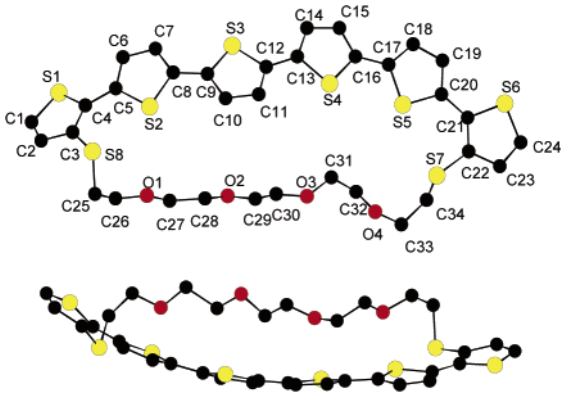

Figure 4. Crystal structure of **6TO$_4$** (hydrogens omitted).

thiophene rings in a syn conformation. This conformation is stabilized by two strong S···S intramolecular interactions [$d(S_5–S_7)$ = 3.174(2) Å; $d(S_2–S_8)$ = 3.266(2) Å] shorter than the sum of the van der Waals radii (3.7 Å). The side view shows that the π-conjugated 6T chain adopts a quasi-planar conformation with, however, a bent geometry imposed by the insufficient length of the polyether loop.

Theoretical calculations based on density functional methods have been performed for dimethylsulfanyl 4T in two different conformations with the Gaussian98 program.[22] Becke's three-parameter gradient-corrected functional (B3lyp) with a polarized 6-31G* basis for all atoms was used to optimize the geometry and to compute the electronic structure at the minima found.

The first minimun calculated conformation corresponds to the isomer shown by the crystal structure in Figure 3, in which the four thiophenes are in a anti−anti−syn (*aas*) conformation. The second minimum conformation anti−syn−anti (*asa*) is based on steric considerations associated with cation complex-

(21) (a) van Bolhuis, F.; Wynberg, H.; Havinga, E. E.; Meijer, E. W.; Staring, E. G. J. *Synth. Met.*, **1989**, *30*, 381. (b) Chaloner, P. A.; Gunatunga, S. R.; Hitchcock P. B. *Acta Crystallogr., Sect. C*, **1994**, *50*, 1941. (c) Pelletier, M.; Brisse, F. *Acta Crystallogr., Sect. C*, **1994**, *50*, 1942.

(22) Frisch, M. J.; Trucks, G. W.; Schlegel, H. B.; Scuseria, G. E.; Robb, M. A.; Cheeseman, J. R.; Zakrzewski, V. G.; Montgomery, J. A., Jr.; Stratmann, R. E.; Burant, J. C.; Dapprich, S.; Millam, J. M.; Daniels, A. D.; Kudin, K. N.; Strain, M. C.; Farkas, O.; Tomasi, J.; Barone, V.; Cossi, M.; Cammi, R.; Mennucci, B.; Pomelli, C.; Adamo, C.; Clifford, S.; Ochterski, J.; Petersson, G. A.; Ayala, P. Y.; Cui, Q.; Morokuma, K.; Malick, D. K.; Rabuck, A. D.; Raghavachari, K.; Foresman, J. B.; Cioslowski, J.; Ortiz, J. V.; Baboul, A. G.; Stefanov, B. B.; Liu, G.; Liashenko, A.; Piskorz, P.; Komaromi, I.; Gomperts, R.; Martin, R. L.; Fox, D. J.; Keith, T.; Al-Laham, M. A.; Peng, C. Y.; Nanayakkara, A.; Gonzalez, C.; Challacombe, M.; Gill, P. M. W.; Johnson, B. G.; Chen, W.; Wong, M. W.; Andres, J. L.; Head-Gordon, M.; Replogle, E. S.; Pople J. A. *Gaussian 98* (Revision A.9); Gaussian Inc.; Pittsburgh, PA, 1998.

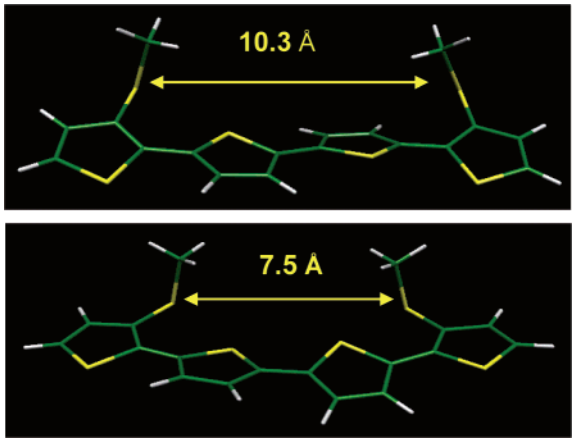

Figure 5. Geometry optimization for dimethylsulfanyl quaterthiophene in *aas* (top) and *asa* (bottom) conformations by the functional density method (Becke3lyp) and Gaussian 98.[22] Bases for calculation are 6-31G* for carbons and sulfur and 6-31G for hydrogens.

Table 4. Computed Values for the Energy Levels for Ground State and Cation Radical of Two Conformations of Dimethylsulfanyl Quaterthiophene

	(*aas*)	(*asa*)	Δ(*aas*) – (*asa*)
HOMO (eV)	−5.08	−5.02	+0.06
Δ*E* (eV)	3.08	3.03	−0.05
λ_{max} (nm)	402	409	+7
cation radical (eV)	−7.91	−7.87	+0.04

ation. In fact, as shown in Figure 5, in the absence of metal cation, the *aas* conformation of the 4T chain imposes a minimal distance of ca. 10.3 Å between the two sulfur atoms at the 3-position of the terminal thiophenes. It is noteworthy that this distance is in excellent agreement with the 10.113 Å found in the crystallographic structure in Figure 3. The formation of a macrocyclic cavity with optimal geometry to fit the cation requires a reduction of this distance to get closer to the ideal situation where the two S atoms would be directly linked by two methylene groups. According to our geometry optimizations, this implies a contraction of the conjugated chain with a shortening of the S···S distance from 10.3 to 7.5 Å, which results in transition from an *aas* to an *asa* conformation

The data in Table 4 shows that the passage from the *aas* to the *asa* conformation leads to a 0.06 eV increase of the HOMO (highest occupied molecular orbital) level and to a comparable decrease of the HOMO−LUMO (lowest unoccupied molecular orbital) gap (Δ*E*) at the fundamental state. This decrease of Δ*E* corresponds to a 7 nm bathochromic shift of the absorption maximum. The calculations also predicts a 0.04 eV increase of the energy of the cation radical, which should correspond to a 40 mV decrease of the oxidation potential associated with the formation of the dicationic state.

Electronic Absorption Spectroscopy. In the absence of metal cation, the electronic absorption spectra of **4TO$_3$**, **4TO$_4$**, and **4TO$_5$** are typical for *n*Ts and show broad structureless absorption bands with maxima at 403 nm (Table 5 and Figure 6).

The similarity of this λ_{max} value with that of the reference open-chain compound **1** (Scheme 1) shows that fixation of the polyether loop at both ends of the 4T chain does not produces major distortion in the conjugated chain. As shown in Figure 6, addition of 1 equiv of Ba^{2+} to a **4TO$_5$** solution produces the

Table 5. Effect of the Complexation of Alkali Earth Metal Cations on the Absorption Maxima for Crown-Annelated Oligothiophenes in 1:1 CH_3CN/CH_2Cl_2

	1[a]	**4TO$_4$**[a]	**4TO$_5$**[a]	**2**[b]	**6TO$_4$**[c]	**6TO$_5$**[d]
+1 equiv of Ba^{2+}	e	413	416	*e*	*e*	*e*
+1 equiv of Sr^{2+}	*e*	410	413	*e*	*e*	*e*
+1 equiv of Pb^{2+}	*e*	415	412	*e*	381, 446	382, 444

[a] Changes are relative to absorption maximum of 403 nm. [b] Changes are relative to absorption maximum of 442 nm. [c] Changes are relative to absorption maxima of 381 and 441 nm. [d] Changes are relative to absorption maxima of 388 and 439 nm. [e] No change.

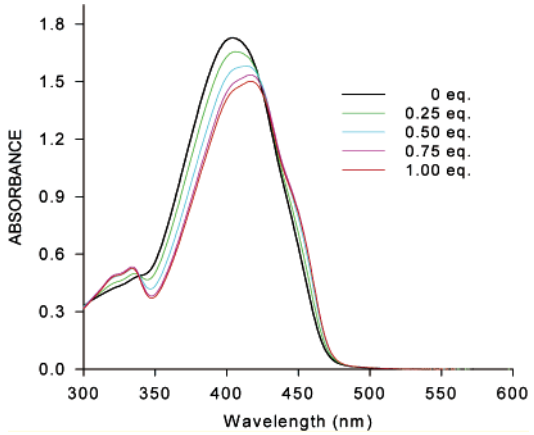

Figure 6. Evolution of the UV−vis spectrum of **4TO$_5$** in 1:1 CH_2Cl_2/CH_3CN versus the number of equivalents of Ba^{2+} added from a 5×10^{-4} M perchlorate solution in CH_3CN.

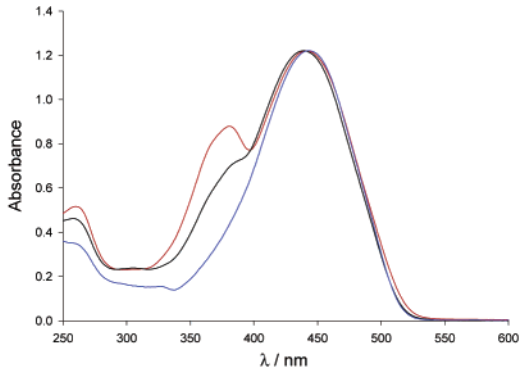

Figure 7. Electronic absorption spectra of **2** (blue), **6TO$_4$** (red), and **6TO$_5$** (black).

emergence of a vibronic fine structure, which indicates that cation complexation results in the rigidification of the conjugated system. On the other hand, the 9−12 nm red shift of λ_{max} shows that complexation produces, as expected, a decrease of the HOMO−LUMO gap. It is noteworthy that the magnitude of these shifts is in good agreement with the theoretically value, thus providing further support to a transition from an *aas* to an *asa* conformation.

Comparison of the electronic absorption spectra of **6TO$_4$** and **6TO$_5$** with that of the open-chain reference compound **2** reveals a small hypsochromic shif of the λ_{max} of the main absorption band from 442 nm for **2** and 441 and 439 nm for **6TO$_4$** and **6TO$_5$**, respectively (Figure 7). These shifts suggest, in agreement with crystallographic data, that the constraint imposed on the 6T chain by the attached polyether loop induces a slight decrease of conjugation.

However, the major difference between the spectrum of the open chain 6T **2** and those of **6TO$_4$** and **6TO$_5$** lies in the

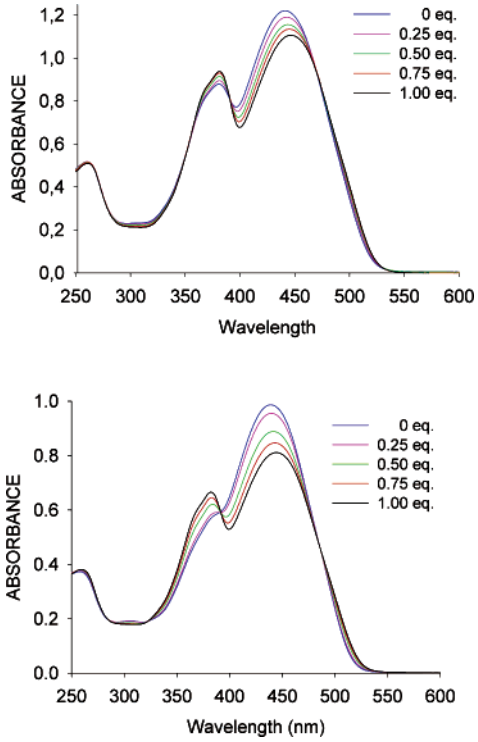

Figure 8. Changes in the UV−vis absorption spectra of **6TO$_4$** (top) and **6TO$_5$** (bottom) in 1:1 CH_2Cl_2/MeCN versus the number of added equivalents of Pb^{2+} (from a 4×10^{-4} M perchlorate solution in CH_3CN).

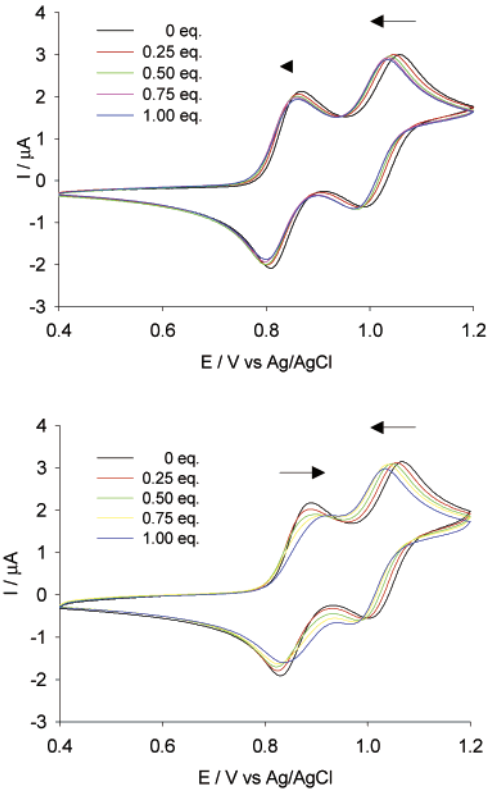

Figure 9. Evolution of the CV of 4**TO$_4$** (top) and **4TO$_5$** (bottom) (1×10^{-4} M) upon addition of Ba^{2+} [added as 1×10^{-3} M $Ba(ClO_4)_2$] in 0.10 M Bu_4NClO_4/1:1 $CH_3CN-CH_2Cl_2$, scan rate 100 mV s^{-1}.

presence of an additional absorption band around 380 nm, which indicates the coexistence of two distinct conjugation lengths. The 440 nm band corresponds to the quasi-planar 6T geometry, whereas the 380 nm band can be attributed to a shorter conjugation length resulting from the formation of a dihedral angle between two parts of the conjugated chain by rotation around a single bond. The maximum at 380 nm suggests that rotation takes place in the middle of the 6T chain, dividing it into two quasi-orthogonal 3T segments. Such an hypothesis is consistent with (i) the absorption maximum expected for an alkylsulfanyl-substituted 3T and (ii) the presence of a single additional absorption band in the short-wavelength region. In fact, a rotation leading to two different conjugated segments (e.g., two and four thiophene rings), should give rise to two new transitions in this spectral region. The larger intensity of the 380 nm band observed for **6TO$_4$** compared to **6TO$_5$** is consistent with a stronger constraint imposed on the 6T chain by the shorter polyether loop.

Addition of metal cation to solutions of **6TO$_4$** and **6TO$_5$** produces a decrease of the 440 nm band with a concomitant increase of the 380 nm one. As shown in Figure 8, these changes occur around an isosbestic point, indicating the interconversion of two distinct species. The largest changes are observed for **6TO$_5$**, in agreement with the larger flexibility allowed the 6T chain by the longer polyether loop. In both cases the strongest effects are observed with Pb^{2+} and are accompanied by a 5 nm red shift of the long wavelength band (Table 5).

Cyclic Voltammetry. The cation-binding properties of the macrocyclic *n*Ts have been investigated by cyclic voltammetry (CV) in 1:1 CH_2Cl_2/CH_3CN in the presence of Ba^{2+}, Sr^{2+}, and Pb^{2+}. Owing to the absence of complexation indicated by ^1H NMR data, **4TO$_3$** was not considered in these experiments and alkali cations were not investigated.

Table 6. Cyclic Voltammetric Data for Crown-Annelated Oligothiophenes[a]

compd	addition[b]	E^0_1, V	ΔE^0_1, mV	E^0_2, V	ΔE^0_2, mV
1		0.98		1.13	
4TO$_3$		0.87		1.10	
4TO$_4$		0.87		1.10	
	$+Ba^{2+}$		−6		−30
	$+Sr^{2+}$		15		−25
	$+Pb^{2+}$		+14		−25
4TO$_5$		0.88		1.08	
	$+Ba^{2+}$		+20		−50
	$+Sr^{2+}$		+30		−30
2		0.85		1.08	
6TO$_4$		0.75		1.05	
6TO$_5$		0.77		1.05	

[a] In 0.10 M Bu_4NClO_4. Scan rate 100 MV s^{-1}, ref Ag/AgCl. [b] After addition of 1 equiv of metal cation.

In the presence of 0.10 M Bu_4NClO_4, the CV of **4TO$_4$** and **4TO$_5$** exhibits two reversible one-electron oxidation processes with redox potentials E^0_1 and E^0_2 at 0.87−0.88 and 1.10 V, corresponding to the successive generation of the cation radical and dication (Figure 9 and Table 6). The E^0_1 and E^0_2 values for the macrocyclic 4Ts are slighly less positive than those for the open-chain reference compound **1**. A similar difference is observed when the E^0_1 and E^0_2 values of **6TO$_4$** and **6TO$_5$** are compared to those of compound **2**. Furthermore, for both series of macrocycles, the lowest E^0_1 and E^0_2 values are obtained for compounds with the shortest polyether loop. Since the reference compounds **1** and **2** are expected to adopt a fully anti conformation in solution, these results suggest that the fixation of the oligooxyethylene loop imposes a preferential conformation with a higher HOMO level on the *n*T chain.

Addition of metal cation has no clear effect on the CV of **6TO$_4$** and **6TO$_5$**. Figure 9 shows the changes induced in the CV of **4TO$_4$** and **4TO$_5$** by addition of Ba^{2+} in the electrolytic medium. Addition of increasing amount of Ba^{2+} to a **4TO$_4$** solution produces a slight negative shift of E^0_1 and a larger negative shift of E^0_2. Similar effects are observed for Sr^{2+} with a larger shift of E^0_1. For Pb^{2+} a quite different behavior is observed since E^0_1 now shifts toward positive potentials. It is noteworthy that the most negative shift observed for Sr^{2+} is correlated with the smallest binding constant indicated by ^{1}H NMR data, whereas the inversion of the shift sign with Pb^{2+} corresponds to a much larger binding constant (Table 2). For **4TO$_5$,** E^0_1 shifts positively with all cations while the shift of E^0_2 remains negative but larger than for **4TO$_4$**.

In both cases, the maximum potential shift is reached after addition of 1 equiv of cation. Although these results confirm the formation of a 1:1 complex between the crown-annelated 4Ts and Ba^{2+}, Sr^{2+}, and Pb^{2+} in close agreement with ^{1}H NMR, mass spectrometry, and optical data, the observed electrochemical behavior is quite unusual.

Cation complexation by redox-active crown ethers containing reversibly oxidizable probes such as, e.g., ferrocene or tetrathiafulvalene (TTF) generally induces a positive shift of the oxidation potential due to electrostatic repulsion between the positive charges of the metal cation and the oxidized probe.[23,24] For macrocycles with two-redox states probes such as TTF, the second oxidation step is unaffected in the presence of metal cations. This invariance is generally attributed to the expulsion of the cation after the first TTF oxidation.

Whereas a similar behavior has also been observed for crown ether-derivatized polythiophenes,[13] examples of redox-active macrocycles undergoing a negative potential shift in the presence of metal cations are scarce. Such behavior has been observed for some TTF cryptands[25] and for some polyether-derivatized poly(thiophenes).[14] In this latter case, spectroelectrochemical experiments have revealed a cation-induced planarization of the poly(thiophene) chain.[14b]

A major difference between most of the redox-active crown ethers reported so far and the present systems lies in the large conformational flexibility of the *n*T chain, which acts at the same time as a part of the macrocyclic cavity and as redox probe. Since the electronic properties of the *n*T chain strongly depend on its geometry, the effects of cation complexation must be discussed in the framework of an interplay between electrostatic interactions and conformationnal changes.

On this basis, the following mechanism can be proposed to interpret the various sets of experimental results (Scheme 2). Metal cation complexation in the neutral state forces the polyether chain to form a macrocyclic cavity, which tends to

Scheme 2

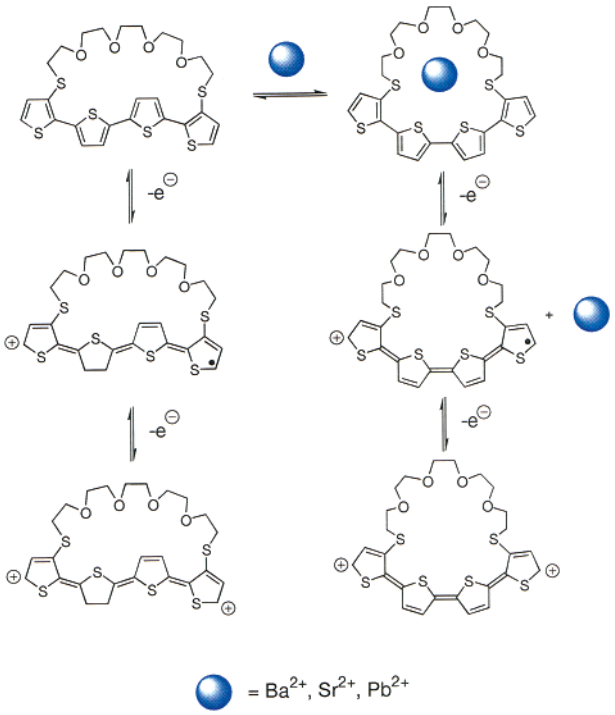

adopt an optimal geometry for cation complexation. As already discussed, this process results in a decrease of the distance between the two sulfide groups, which in turn induces a transition in the 4T chain from an *aas* to an *asa* conformation more easily oxidizable. When the binding constant is low, as for **4TO$_4$** and Ba^{2+} or Sr^{2+} (Table 2), repulsive electrostatic interactions are weak and geometrical effects predominate, inducing a red shift of λ_{max} and a negative shift of E^0_1. In contrast, for **4TO$_5$** the larger binding constant ($K^0 > 10^5$) suggests a better match between the geometry of the macrocyclic cavity and metal cation. In addition to an enhanced Coulombic repulsion between positive charges, cation complexation results in a decrease of the electron-releasing effect of the sulfur atoms connected to the thiophene rings. These combined effects produce a positive shift of E^0_1 larger than for **4TO$_4$**. Although conformational changes that should produce a decrease of E^0_1 still occur [as demonstrated by the red shift of λ_{max} (Table 3)], the net effect is nevertheless a positive shift of E^0_1.

Oxidation of π-conjugated systems with a nondegenerate ground state such as polythiophene to the cation radical state is accompanied by a transition from an aromatic to a quinoid structure.[26] Consequently, once the first oxidation stage is reached, the π-conjugated system is locked into a fixed conformation. Thus, if metal cation complexation imposes a preferential conformation to the neutral *n*T chain, this conformation is retained after the first oxidation step. Since, as suggested by UV−vis and CV data, the presence of a metal cation in the macrocycle imposes a conformation of higher HOMO level to the 4T chain, it follows that even after cation expulsion consecutive to the first oxidation step, the 4T chain retains the *asa* conformation induced by the transient stay of the metal cation in the macrocycle. Then, the second oxidation process starts from an *aas* conformation of the 4T chain in the absence

(23) Recent reviews: (a) Boulas, P. L. M.; Gomez-Kaifer, M.; Echegoyen, L. *Angew. Chem., Int. Ed.* **1998**, *37*, 216. (b) Beer, P. D.; Gale, P. A.; Chen, G. Z. *J. Chem. Soc., Dalton. Trans.* **1999**, 1897. (c) Bronsted Nielsen, M.; Lomholt, C.; Becher, J. *Chem. Soc. Rev.* **2000**, *29*, 153.

(24) (a) Hansen, T. K.; Jørgensen, T.; Stein, P. C.; Becher, J. *J. Org. Chem.* **1992**, *57*, 6403. (b) Bryce, M. R.; Batsanov, A. S.; Finn, T.; Hansen, T. K.; Howard, J. A. K.; Kamenjicki, M.; Lednev, I. K.; Ascher, S. A. *Chem. Commun*. **2000**, 295. (c) Le Derf, F.; Mazari, M.; Mercier, N.; Richomme, P.; Levillain, E.; Becher, J.; Garin, J.; Orduna, J.; Gorgues, A.; Sallé, S. *Chem. Commun*. **1999**, 1417. (d) Le Derf, F.; Mazari, M.; Mercier, N.; Levillain, E.; Trippé, G.; Riou, A.; Richomme, P.; Becher, J.; Garin, J.; Orduna, J.; Gallego-Planas, N.; Gorgues, A.; Sallé, M. *Chem. Eur. J.* **2001**, *7*, 447.

(25) Gasiorowski, R.; Jørgensen, T.; Moller, J.; Hansen, T. K.; Pietraszkiewicz, M.; Becher, J. *Adv. Mater*. **1992**, *4*, 568.

(26) (a) Brédas, J. L.; Thémans, B.; Fripiat, J. G.; André, J. M.; Chance, R. R. *Phys. Rev. B* **1984**, *29*, 6761. (b) Patil, A. O.; Heeger, A. J.; Wudl, F. *Chem. Rev.* **1988**, *88*, 183.

of metal cation and from an *asa* conformation in the other case (Scheme 2). Theoretical calculations performed on the dimethylsulfanyl 4T cation radical shows that the energy of the *asa* conformation is ca. 0.04 eV higher than for the *aas* conformation (Table 4). This result nicely agrees with the 30−50 mV negative shift of E^0_2 observed in the presence of metal cation.

Conclusion

Crown-annelated oligothiophenes have been synthesized by the thiolate protection/deprotection method. Analysis of the ionophoric properties of the macrocycles by ^{1}H NMR, mass spectrometry, UV−vis spectroscopy, and cyclic voltammetry gives consistent results which show that the compounds do not complex alkali cations but show moderate to good binding properties for alkali-earth cations. The cation-binding constant increases with the length of the polyether chain, whereas shorter polyether loops impose a stronger constraint to the conjugated system.

^{1}H NMR, optical, electrochemical, and theoretical results provide conclusive evidence showing that cation complexation induces a conformational transition in the oligothiophene chain. This process can be utilized either as a means to achieve a mechanical control of the electronic properties of the π-conjugated system or as a source of molecular actuation, thus contributing to enrich the toolbox for the emerging field of molecular machines and motors.

Extension of this concept to other annelated oligothiophenes containing photostimulable driving groups is now underway and will be reported in forthcoming papers.

Supporting Information Available: Experimental procedures for the synthesis of all compounds and X-ray crystallographic files for **6TO$_4$** and **4TO$_4$** (PDF). This information is available free of charge via the Internet at http://pubs.acs.org.

JA026819P